Available online at www.sciencedirect.com
SCIENCE DIRECT
Composites: Part B 37 (2006) 365–378
composites Part B: engineering
www.elsevier.com/locate/compositesb

Effectiveness of z-pins in preventing delamination of co-cured composite joints on the example of a double cantilever test

Larry W. Byrd[a,*], Victor Birman[b]

[a]Air Force Research Laboratory, AFRL/VASM, Building 65, 2700 D Street, Wright-Patterson Air Force Base, OH 45433, USA
[b]Engineering Education Center, University of Missouri-Rolla, One University Boulevard, St Louis, MO 63121, USA

Received 5 January 2005; accepted 16 May 2005
Available online 27 December 2005

Abstract

The effectiveness of z-pins in co-cured joints is illustrated on the model of a composite double cantilever beam (DCB) subject to a standard fracture toughness test. A comprehensive solution is presented in the paper accounting for a broad spectrum of issues that affect the problem. They include the accurate evaluation of the rotational constraint provided by the intact section of DCB, possible transverse shear deformation in the delaminated section, and effects of uniform and nonuniform temperature on the response. A simple criterion for the effectiveness of z-pins in co-cured joint is introduced and its application is illustrated on numerous examples. As follows from the analysis, z-pinning is an effective method of enhancing delamination resistance of composite joints. Even a very small volume fraction of z-pins (less than 1.5%) may arrest delamination in co-cured composite joints.

Keywords: A. Fracture toughness; Laminates; Polymer matrix composites (PMCS)

1. Introduction

Delamination cracks originating from the edge are recognized as the principal cause of damage and failure in bonded adhesive and co-cured joints. Z-Pins, i.e. small-diameter cylindrical rods embedded in the composite material and oriented perpendicular to the layer interface, represent a possible method of arresting these cracks. Extensive studies that illustrated beneficial effects of z-pins on various aspects of the behavior of composite structures have been published [1–6]. In particular, this method may be effective in enhancing fracture and fatigue resistance of co-cured joints between composite skin and stiffeners similar to the joint depicted in Fig. 1.

The advantages associated with using z-pins to reduce or prevent delamination tendencies in polymeric matrix composites have been documented in numerous studies. For example, Freitas et al. [1,7] illustrated that a 1.9% volume fraction of carbon z-pins can increase Mode I fracture toughness of laminates by a factor of 18 with only modest reduction in in-plane tensile strength. Inclined at 45°, z-pins have also been shown beneficial for lap shear specimens [8]. In the present study, the effectiveness of z-pins is estimated on the example of a standard DCB test prescribed for composite adhesive joints (though an adhesive layer is not used in co-cured joints). A typical setup of the test is presented in Fig. 2.

One of the previous solutions considered by the authors employed the analysis of a co-cured z-pinned DCB based on modeling the effect of a limited rotational constraint of the intact part of the beam (see Fig. 3, $x>0$) through the introduction of an elastic foundation [9]. Such approach to modeling the constraint that affects deformations of the delaminated 'legs' of DCB was originally proposed by Kanninen [10,11] and Gehlen et al. [12] for studies of Mode I fracture in the joints without z-pins. It was further extended to transversely isotropic materials by Williams [13] and to angle-ply laminates by Ozdil and Carlsson [14]. Penado [15] used the same approach to incorporate the effect of an adhesive layer between the two halves of the beam. The authors presented a new method of the solution where the elastic rotational constraint at the tip of the crack was analytically evaluated from the elasticity analysis of the intact section of DCB [16]. Subsequently, the analysis of

* Corresponding author.

1359-8368/$ - see front matter © 2005 Elsevier Ltd. All rights reserved.
doi:10.1016/j.compositesb.2005.05.019

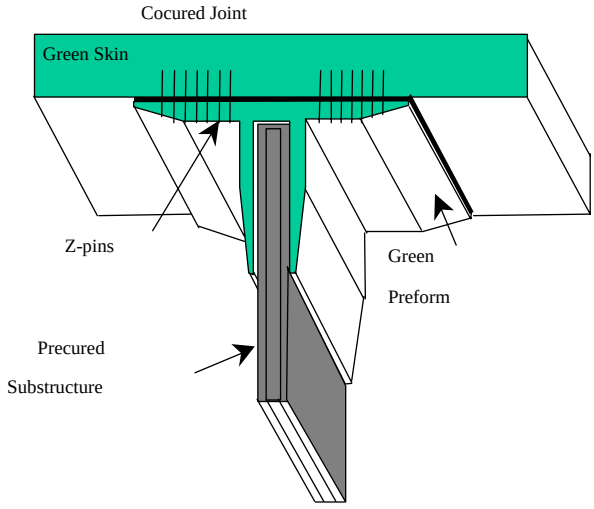

Fig. 1. Co-cured z-pinned joint between the skin and stiffener.

the delaminated section (section 1 in Fig. 3) was carried out without difficulties.

In both previous papers [9,16], the effect of z-pins was introduced through an equivalent elastic foundation (Fig. 3). This approach was first suggested by Mabson and Deobald [6], who based it on the analysis of Li [17]. The application of this approach as well as the effect of z-pins on the properties of the material are further discussed in the present paper.

Elevated temperature may have a noticeable effect on fracture of z-pinned co-cured joints. The present paper provides a methodology of the analysis of the effect of z-pins on the integrity of z-pinned co-cured joints for the case of a nonuniform temperature introducing a concept of 'insulated crack' in the DCB test setting. Furthermore, a numerical analysis of the effect of the z-pin-composite interfacial shear strength varying as a result of a uniform temperature on Mode I fracture is presented. A large effect of the interfacial shear strength on the integrity of joints undergoing Mode I loading observed in numerical examples

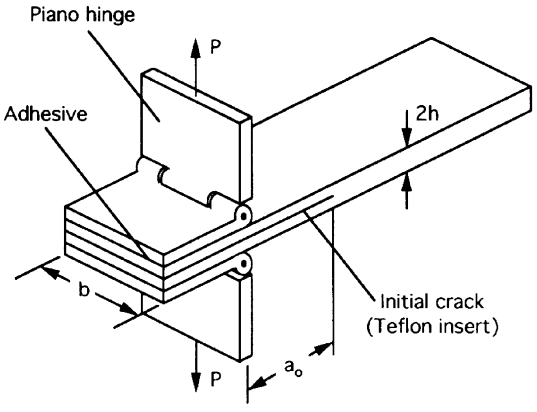

Fig. 2. Schematic illustration of the DCB test, according to ASTM 5528 and ASTM, D 5528-01.

led to the recommendation to employ artificially uneven surfaces of z-pins to maximize their resistance to pullout.

The analysis of the integrity of z-pinned joints may not be successfully carried out using a fracture toughness approach since fracture toughness is affected by the bridging effect of z-pins [8]. A criterion of failure of z-pinned co-cured joints based on the analysis of deflections of the delaminated section of a representative DCB is introduced in the present study. This convenient criterion enables us to estimate the effectiveness of z-pins in the joints, including the case where temperature is present.

It is useful to recall here the solution for the critical strain energy release rate for Mode I fracture of DCB specimens with or without z-pins that remain within the elastic range:

$$G_{\mathrm{IC}} = \frac{P_{\mathrm{c}}^2}{2b}\frac{\mathrm{d}C}{\mathrm{d}a} \tag{1}$$

where P_{c} is the fracture load, is the width of the specimen, and $\mathrm{d}C/\mathrm{d}a$ is the rate of change of the compliance per unit crack growth. Difficulties in evaluating $\mathrm{d}C/\mathrm{d}a$ prevent us from formulating an analytical closed-form solution for the strain energy release rate or fracture toughness.

2. Analysis of the effect of z-pins

The presence of z-pins affects a DCB through two mechanisms. First of all, z-pins affect stiffness in both axial (x) and transverse (z) directions (see Fig. 3 for the coordinate axes). The stiffness of z-pins in the transverse (z) direction is much higher than the stiffness of the joined composite material, affecting the transverse stiffness of the specimen. The effect of z-pins on the stiffness in the axial (x) direction is smaller since the pins work similar to fibers in transversely loaded laminae.

The properties of z-pinned materials in both axial and transverse directions can be evaluated by one of micromechanical theories. The presence of z-pins is treated as if these pins were 'fibers' embedded within an orthotropic 'matrix' represented by the composite material of the layers. For example, the mechanics of materials approach to the evaluation of the properties of a composite material is applicable. A 'simplified' micromechanical model can be employed to evaluate the moduli [18]:

$$E_{xj} = \frac{E_{1j}}{1-\sqrt{V_{\mathrm{p}}}\left(1-\frac{E_{1j}}{E_{x\mathrm{p}}}\right)}, \qquad G_{xzj} = \frac{G_{13j}}{1-\sqrt{V_{\mathrm{p}}}\left(1-\frac{G_{13j}}{G_{\mathrm{p}}}\right)} \tag{2}$$

where E_{1j} is the modulus of the pristine jth layer (without the z-pins) in the axial (x) direction, $E_{x\mathrm{p}}$ is the transverse modulus of the pin material, G_{13j} is the transverse shear modulus of the pristine composite material, G_{p} is the shear

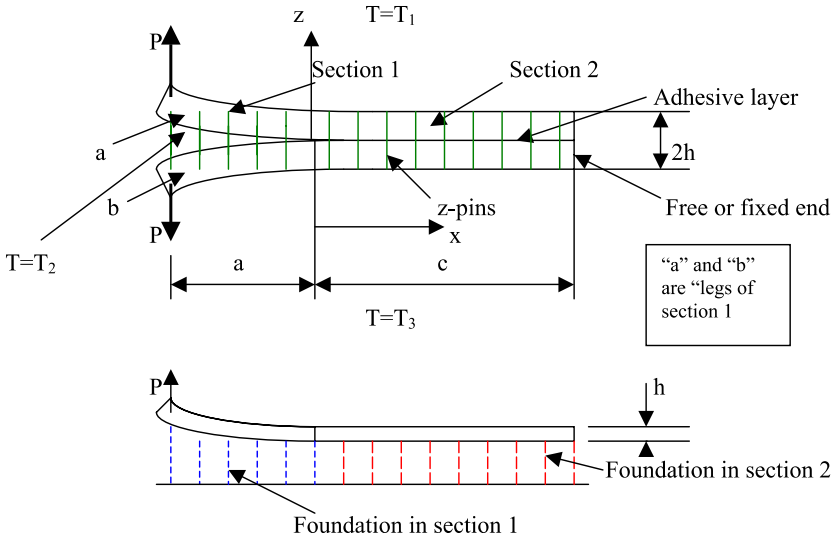

Fig. 3. DCB with z-pins loaded in mode I and the model used in the analysis based on modeling the rotational stiffness of Section 2 through the introduction of an elastic foundation. The case of a nonuniform temperature $T=T_i$ is considered in the paper.

modulus of the pin material, and V_p is the volume fraction of z-pins.

The modulus of the jth layer in the z-direction can be obtained by the rule of mixtures as

$$E_{zj} = V_p E_{zp} + (1 - V_p) E_{3j} \tag{3}$$

where E_{3j} is the modulus of the composite material in the thickness direction and E_{zp} is the corresponding modulus of the pin material.

The Poisson ratios can be evaluated from

$$\nu = (1 - V_p)\nu_{czxj} + V_p \nu_p, \qquad \nu_{xzj} = \nu_{zxj} \frac{E_{xj}}{E_{zj}} \tag{4}$$

where ν_{czxj} is the Poisson ratio of the jth layer without z-pins and ν_p is the Poisson ratio of the pin material.

A more elaborate micromechanical formulation based on the improved mechanics of materials approach, the semi-empirical theory of Halpin–Tsai or advanced theories (Mori–Tanaka, method of cell, etc.) is also possible. However, they are not employed in this study since a relatively simple micromechanics outlined above provides qualitatively accurate results.

In addition to the effect of z-pins on the properties of the material of DCB, it should be noted that as z-pins are pulled out of the delaminated 'leg' of the specimen, as shown in Fig. 3, the volume previously occupied by z-pins is empty. Therefore, the stiffness of a leg of DCB pulled by the applied force is a function of the x-coordinate. This phenomenon could greatly complicate the analysis. However, it was found that even if the ratio of the modulus of the pin to the corresponding modulus of the layer is infinite, the moduli E_{xj} and G_{xzj} cannot exceed the moduli of the pristine layer by more than the factor of 1.11 ($V_p=1\%$) or 1.25 ($V_p=4\%$). The lower limit of variations of the moduli (pin pullout) was defined as the corresponding modulus of the pristine layer multiplied by the factor of 0.99 ($V_p=1\%$) or 0.96 ($V_p=4\%$).

As follows from this discussion, the range of variations of moduli E_{xj} and G_{xzj} of a z-pinned specimen is narrow. Following a similar approach, it can be shown that the variations in the Poisson ratios also remain small (besides, the effect of these ratios on the solution for a beam is insignificant). As was shown in the papers on mixed-mode fracture of z-pinned specimens [8] and in the recent work on Mode I fracture [9,16], z-pins suppress the opening mode so that the anticipated amount of pullout (and the related depth of the affected zone) cannot be large, unless the specimen begins to fail. In conclusion, it is possible to use the values of moduli accounting for the presence of z-pins and neglecting a small reduction in the stiffness due to their partial pullout.

The reaction of z-pins in the delaminated section of DCB can be evaluated following the approach used by Mabson and Deobald [6] and Li [17]. The nonlinear pullout force-displacement response of z-pins includes the initial linear relationship corresponding to a limited motion of the pins relative to the composite material adjacent to the crack plane. After the entire interface between the pin and matrix is affected, the force applied by the pin to the matrix decreases, yielding the following pressure on the delaminated section [6]:

$$p = K_0 - K_1 w, \qquad K_0 = 2V_p \tau l_p / r, \qquad K_1 = 4V_p \tau / r \tag{5}$$

where l_p and r are the pin embedded length (in this paper it is assumed equal to the thickness of the delaminated section h) and radius, respectively, and τ is the interfacial shear strength. The initial ascending linear force–displacement response is often neglected since it corresponds to very small deflections. In this case, Eq. (5) represents the reaction of the pins in Section 1 in a DCB specimen shown in Fig. 3.

Note that Eq. (5) could be derived by assuming a constant frictional bond that is independent of the amount of sliding [17].

If z-pins are pulled from one of the legs, the expressions for the pressure applied by them to each leg remain the same, i.e. (5). The deflections of both legs are still equal to each other. This can be explained by observing that the equilibrium of tensile forces in a z-pin cross-section pulled out of the legs requires the same force to be applied by the pin to both legs. Therefore, each leg experiences the same deformation as long as it is subject to the same externally applied load.

If the thickness of delaminated legs is different or if the loads applied to the legs differ, as is the case where DCB is subject to a nonuniform through the thickness temperature, deflections of the legs are not the same, i.e. $w_a \neq w_b$ in Fig. 3. In this case, the second term in the expression for p in Eq. (5) becomes $K_1 w = 2V_p\tau(w_a + w_b)/r$.

2.1. Analysis of rotational constraint of the intact section of DCB with z-pins

Consider a unit-width DCB specimen subject to 'opening' forces at the delaminated end as shown in Fig. 3. The previous research by Kanninen [10] and later investigators was based on modeling the rotational constraint of the intact section (section 2 in Fig. 3) through the introduction of an elastic foundation. Although rather arbitrary, such approach yielded good agreement with experimental results. However, the accuracy of the solution depended on the appropriate choice of the coefficient of the elastic foundation. The shortcomings of this approach were eliminated in the recent paper by Birman and Byrd [16], where the rotational stiffness of the intact part of DCB was derived through the elasticity solution obtained by assumption that the changes in the thickness of the intact part of the beam are negligible. The validity of this assumption is illustrated in the present analysis.

The upper section (half-thickness) of the intact part and the coordinate system employed in the analysis are shown in Fig. 4. The section is subject to a moment M (stress couple, for a unit-width beam) that is replaced with a couple of forces (stress resultants) $N = M/h$ that cause shear deformations of the section.

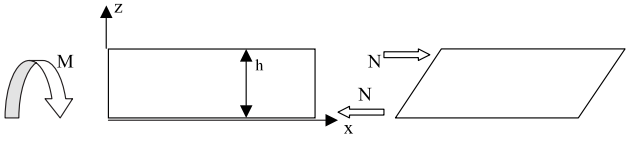

Fig. 4. Computational model of the intact section (section 2 in Fig. 3, i.e. half-thickness of the intact part of DCB). The applied moment and the undeformed section are shown on the left. A couple of forces equivalent to the applied moment and the deformed section are shown on the right.

The analysis is based on the following assumptions:

1. All layers of the section are perfectly bonded to each other.
2. Vertical displacements at the interface of the section $z = 0$ are absent as a result of symmetry of the problem.
3. The length of the section is sufficiently large compared to the depth to assume that the section is semi-infinite. This is based on the previous research that showed that the length of delamination cracks corresponding to either their arrest due to the action of z-pins or failure of DCB is small, i.e. the intact section is quite long compared to the delaminated section [9,16].
4. Z-Pins do not experience pullout in the intact part of DCB. Accordingly, shearing stresses along the pin–composite interface that are associated with pin pullout are not activated in the intact section.

The analysis is conducted by the Rayleigh–Ritz method. The horizontal and vertical displacements of the section are assumed in the form

$$u = U\,\mathrm{e}^{-\omega x}\cos\frac{\pi z}{h}, \qquad w = W\,\mathrm{e}^{-\omega x}\sin\frac{\pi z}{2h} \tag{6}$$

where ω is a decay parameter that has to be determined.

The displacements in the form (6) satisfy the boundary conditions of the problem:

$$\begin{aligned} &z = 0: \quad w = 0 \\ &x \to \infty: \quad u \to 0, w \to 0 \end{aligned} \tag{7}$$

The total energy of the section of width b subject to a couple of forces N is

$$\Pi = \frac{b}{2}\int_{x=0}^{x=\infty}\int_{z=0}^{z=h}(Q_{11}\varepsilon_x^2 + Q_{33}\varepsilon_z^2 + 2Q_{13}\varepsilon_x\varepsilon_z + Q_{55}\gamma_{xz}^2)\mathrm{d}z\mathrm{d}x - 2NU \tag{8}$$

where Q_{ij} are transformed reduced stiffnesses that are obtained from the reduced stiffnesses in the material principal axes through standard transformation equations [19].

The last term in Eq. (8) represents the energy of applied forces, U being the horizontal displacement of the points of force application.

The strains in Eq. (8) are the following functions of displacements:

$$\varepsilon_x = u_{,x}, \qquad \varepsilon_z = w_{,z}, \qquad \gamma_{xz} = u_{,z} + w_{,x} \tag{9}$$

The integral in Eq. (8) can be evaluated numerically, on the layer to layer basis. In the case of an orthotropic or quasi-isotropic laminate, a closed form solution is available that is illustrated below.

For an orthotropic or quasi-isotropic composite material of DCB where the stiffnesses are independent of the

z-coordinate, the substitution of Eq. (9) into Eq. (8) and integration yields

$$\Pi = \frac{b}{8}\left(cQ_{11} + \frac{\pi^2}{c}Q_{55}\right)U^2 + \frac{b}{8}\left(cQ_{55} + \frac{\pi^2}{4c}Q_{33}\right)W^2 + \frac{b}{6}(4Q_{55} - Q_{13})UW - 2NU \tag{10}$$

where $c=\omega h$. Note that this result remains valid in the presence of z-pins as long as their contribution to the stiffness is accounted for.

Minimization of the total energy given by Eq. (10) with respect to independent variables c, U, W yields the following system of three nonlinear algebraic equations:

$$\left(Q_{11} - \frac{\pi^2}{c^2}Q_{55}\right)U^2 + \left(Q_{55} - \frac{\pi^2}{4c^2}Q_{33}\right)W^2 = 0,$$

$$\frac{b}{4}\left(cQ_{11} + \frac{\pi^2}{c}Q_{55}\right)U + \frac{b}{6}(4Q_{55} - Q_{13})W = 2N, \tag{11}$$

$$\frac{1}{3}(4Q_{55} - Q_{13})U + \frac{1}{2}\left(cQ_{55} + \frac{\pi^2}{4c}Q_{33}\right)W = 0$$

In addition to a numerical solution of Eq. (11), a rather accurate result can be obtained using the value of c obtained in [16] by assumption that displacements in the z-direction are negligible, i.e. neglecting w. As was shown in [16], in this case,

$$c_1 = \pi\sqrt{\frac{Q_{55}}{Q_{11}}} \tag{12}$$

where the subscript in the left side implies that this value can be used as the first iteration.

Using $c=c_1$ in the last two Eq. (11) that were obtained by minimization of the total energy with respect to U, W results in the solution for these variables. Subsequently, the updated value of can be determined from the first Eq. (11):

$$c_2 = \pi\sqrt{\frac{Q_{55}U^2 + \frac{1}{4}Q_{33}W^2}{Q_{11}U^2 + Q_{55}W^2}} \tag{13}$$

As follows from numerical examples, a difference between c_1 and c_2 is small since $W^2 \ll U^2$. Accordingly, a sufficiently accurate solution is available using the first iteration for c, i.e. Eq. (12).

The rotational stiffness provided by the intact section at the end $x=0$ is now available from

$$K = \frac{Nh}{2U/h} = \frac{Nh^2}{2U} \tag{14}$$

Note that the rotation defined in Eq. (14) as $2U/h$ differs from the average shear strain in the cross-section $x=0$. This strain is obtained from

$$\gamma_{av} = \left|\frac{1}{h}\int_0^h \gamma_{xz}(x=0)\mathrm{d}z\right| = \frac{2U}{h} + \frac{2\omega W}{\pi} \tag{15}$$

The substitution of $c=c_1$ yields

$$\gamma_{av} = \frac{2U}{h}\left(1 + \frac{W}{U}\sqrt{\frac{Q_{55}}{Q_{11}}}\right) \tag{16}$$

As follows from numerical examples, the second term in the brackets is small compared to unity, so that the average shear strain is close to the rotation of the cross-section.

It is convenient to represent a closed form expression for the rotational stiffness based on the first iteration described above. Using the solution of the last two Eq. (11) with $c=c_1$, one obtains from Eq. (14)

$$K = \frac{\pi h^2 b}{8} \times \sqrt{Q_{11}Q_{55}}\left[1 - \frac{2}{9\pi^2 Q_{55}}\frac{(4Q_{55} - Q_{13})^2}{Q_{55} + \frac{\pi}{4}\sqrt{\frac{Q_{11}}{Q_{55}}}Q_{33}}\right] \tag{17}$$

It is interesting to compare this expression with the result obtained without accounting for the displacements in the z-direction [16]:

$$K(w=0) = \frac{\pi h^2 b}{8}\sqrt{Q_{11}Q_{55}} \tag{18}$$

If the second term in the square brackets in Eq. (17) is negligible compared to unity, this equation converges to Eq. (18). A comparison between two values of rotational stiffness obtained from Eqs. (17) and (18) is presented in the paragraph on the numerical analysis considering the ratio

$$r = \frac{K}{K(w=0)} = 1 - \frac{2}{9\pi^2 Q_{55}}\frac{(4Q_{55} - Q_{13})^2}{Q_{55} + \frac{\pi}{4}\sqrt{\frac{Q_{11}}{Q_{55}}}Q_{33}} \tag{19}$$

2.2. Analysis of deformations and failure of delaminated section of DCB by the first-order shear deformation theory (FSDT)

One of the delaminated sections and the associated coordinate system are shown in Fig. 5. The section has been turned by 180° compared to Fig. 3, for the convenience of the analysis.

The section is analyzed using the first-order shear deformable theory. The strains in the shear-deformable section are given by

$$\varepsilon_x = z\psi_{,x}, \qquad \gamma_{xz} = \psi + \bar{w}_{,x} \tag{20}$$

where ψ is the rotation of the element that was perpendicular to the undeformed middle axis prior to deformation and is

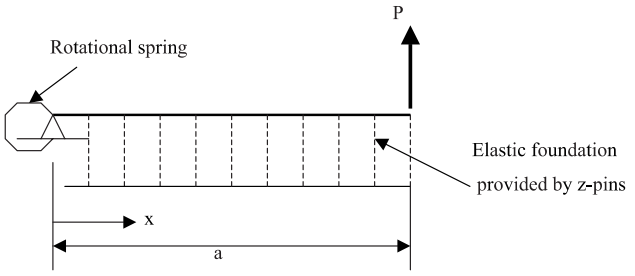

Fig. 5. Computational model of the delaminated section of DCB (section 1 in Fig. 3).

the deflection (in the z-direction). It is emphasized that contrary to the analysis of the intact section conducted above, $\bar{w}$ is a deflection of the neutral axis of the section, rather than a displacement within the section. Axial displacements are equal to zero if the section is symmetrically laminated about its middle axis (the case considered here).

If z-pins at the end of the delaminated section are completely pulled out, the reaction of the elastic foundation becomes equal to zero. This situation is not considered here since as was shown in [9,16], the onset of z-pin pullout can be identified with failure.

The boundary conditions that have to be satisfied are:

$$\begin{aligned} &\bar{w}(0) = 0, \qquad M(0) = -K[\psi(0) + \bar{w}_{,x}(0)], \\ &M(a) = 0, \qquad Q(a) = P \end{aligned} \tag{21}$$

where P is the applied force, while the stress couple and the transverse shear stress resultants are given by

$$M = D\psi_{,x}, \qquad Q = \kappa A(\bar{w}_{,x} + \psi) \tag{22}$$

In Eq. (22), D and A are the bending and extensional stiffness of the leg, respectively, and κ is the shear correction factor.

A convenient feature of the Rayleigh–Ritz method employed in this analysis is that it requires only the satisfaction of kinematic boundary conditions, i.e. the first Eq. (21). This condition is satisfied by the following choice of displacements:

$$\bar{w} = \sum_n W_n \sin\frac{n\pi x}{2a}, \qquad \psi = F_0 + \sum_n F_n \cos\frac{n\pi x}{2a} \tag{23}$$

where W_n, F_0, F_n are coefficients that have to be determined. Note that a different choice of the expressions for deflection and rotation using the power series was considered in [16]. In either case, the solution of the problem is straightforward. In particular, if the analysis is limited to $n=1$, the problem is reduced to finding three coefficients from the set of three algebraic nonlinear equations available using the Rayleigh–Ritz method:

$$\begin{bmatrix} a_{11} & a_{12} & a_{13} \\ a_{21} & a_{22} & a_{23} \\ a_{31} & a_{32} & a_{33} \end{bmatrix} \begin{Bmatrix} F_0 \\ F_1 \\ W \end{Bmatrix} - \begin{Bmatrix} 0 \\ 0 \\ b_3 \end{Bmatrix} W^2 = \begin{Bmatrix} 0 \\ 0 \\ P/b \end{Bmatrix} \tag{24}$$

The coefficients in (24) are easily available and omitted here for brevity. However, a simple illustration is sufficient to conclude than the slender-beam approximations are adequate in most applications, as long as we are concerned with deformations, rather than the stress analysis.

To illustrate the limits of applicability of a slender beam theory, consider an isotropic cantilever of length L without an elastic foundation subject to the load P applied at the free end. The deflections of the free end with and without shear deformation effects are given by

$$w' = \frac{PbL^3}{3EI} + \frac{Pba}{\kappa Gbh}, \qquad w'' = \frac{PbL^3}{3EI} \tag{25}$$

respectively. In Eq. (25), all notations are self-evident, and the shear correction factor used to obtain the second term in the first Eq. (25) is $\kappa = 5/6$.

The ratio of displacements given by Eq. (25) is

$$R = \frac{w'}{w''} = 1 + \frac{3}{10}\frac{E}{G}\left(\frac{h}{a}\right)^2 \tag{26}$$

For example, if the allowable inaccuracy using the slender beam theory is 10%, i.e. $R \le 1.1$, it is evident that for the ratio $E/G = 3$, $a \ge 3\,h$, while if $E/G = 10$, $a \ge 1.85\,h$.

The papers [9,16] illustrated that the lengths of cracks corresponding to either the arrest or the failure are typically larger than the limits evaluated in the previous paragraph. Therefore, the slender beam theory provides an adequate prediction regarding the failure or arrest of delamination cracks in the presence of z-pins in most situations. This conclusion also follows from the comparison of the results obtained for representative z-pinned DCB analyzed by FSDT and the slender beam theory. Accordingly, the latter theory is employed below for the case where the specimen is subject to a combined action of the forces P and a uniform temperature.

2.3. Analysis of the effect of a nonuniform temperature

Co-cured z-pinned joints of aerospace structures will likely be used in a high-temperature environment characterized by the range of temperature from 650–1200°C (≈1200–2200°F). An elevated temperature will often be applied on one of the surfaces, while the opposite surface of the joined component will be at a lower temperature. Accordingly, the problem of a nonuniform temperature distribution through the thickness of the joint represents a major interest. Note that the issue of residual thermal stresses is also important but it is usually relevant in the micromechanical analysis concerned with the integrity of

the pin-composite interface (this problem is not considered here).

An elevated temperature that is uniform over the surface of the component but varies in the thickness direction produces stress couples and stress resultants associated with both the nonuniform temperature distribution as well as the nonuniform distribution of the properties of the constituent materials through the thickness of the joint. In a partially delaminated joint modeled by DCB the stress resultants are equal to zero since there is no constraint against axial displacements. However, stress couples are present and they cause bending of the intact section of DCB as well as the delaminated legs of the specimen. Even if the external forces are not applied to the joint or DCB, thermally induced deformations appear as a result of thermal stress couples.

As follows from the numerical solution of the heat transfer problem, variations of temperature in the planes perpendicular to z-pins at the macromechanical level are negligible compared to those in the thickness direction of the laminate. Therefore, it is possible to limit the heat transfer analysis to the one-dimensional problem using the values of the conductivities accounting for the presence of z-pins in composite layers (the rule of mixtures is applicable in this case). If the effect of temperature on the conductivity in the thickness direction is accounted for, the problem becomes nonlinear. For example, as was shown by Birman [20], if the conductivity is a linear function of temperature, i.e.

$$k = k_0 + k_1 T \tag{27}$$

temperature is distributed through the material according to

$$T = -\frac{k_0}{k_1} + \sqrt{C_1 z + C_0} \tag{28}$$

where C_i are constants available from the thermal boundary conditions. In the case where a perfect thermal boundary is maintained between the layers that have the same conductivity in the thickness direction the previous relationship would remain valid in a co-cured laminated joint.

The analysis of a representative DCB can be conducted using a concept of 'insulated crack', i.e. assuming that there is no heat loss from the side surfaces of the beam and temperature remains constant within the entire volume occupied by the crack. This implies that there is no heat transfer out of the crack to the left of the cross-section $x=-a$ of the specimen (Fig. 3). Although 'insulated crack' is physically meaningless for DCB, the assumption of a constant temperature within a delamination crack reflected in this concept is accurate in engineering applications. This enables us to make the following observations.

The intact section (Section 2) will bend as a result of a nonuniform temperature, resulting in a rotation of the cross-section $x=0$. This rotation will cause the same rotation of both legs of Section 1, i.e. there are no associated relative displacements of the legs at the cross-section $x=-a$. However, even if $T_2=(T_1+T_3)/2$, the property degradation in two legs of Section 1 is different, as the magnitude of temperature in two legs differs. Accordingly, thermally induced bending moments in these sections and the corresponding deformations are different as well. Moreover, a different degree of degradation of material constants in two legs causes a different correction to deformations produced by the applied forces. Note that a degradation of the material in Section 2 will affect the elastic clamping coefficient at the cross-section $x=0$.

The first step of the solution is determining elastic clamping provided by Section 2 to delaminated Section 1. As follows from the analysis at a room temperature, Eq. (18) is adequate. However, the stiffness coefficients in this formula are now affected by temperature. Therefore, the solution has to be adjusted accordingly.

As follows from the solution at the room temperature, the total energy of Section 2 subject to a bending couple at the edge, as shown in Fig. 4, can be obtained neglecting deformations in the thickness direction, so that

$$\Pi = \frac{1}{2}\int_{x=0}^{x=\infty}\int_{z=0}^{z=h}(Q_{11}(z)\varepsilon_x^2 + Q_{55}(z)\gamma_{xz}^2)\mathrm{d}z\mathrm{d}x - 2NU \tag{29}$$

where $Q_{ii}(z)$ should be specified, accounting for a distribution of temperature and the effect of temperature on the material constants. Eq. (29) is written for the section subject to mechanical loading that causes shear and rotation of the cross-section $x=0$, while thermally-induced deformations are not considered (these deformations result in a rotation of the cross-section $x=0$, but they do not affect the elastic restraint).

The strains in Eq. (29) are

$$\varepsilon_x = u_{,x}, \qquad \gamma_{xz} = u_{,z} \tag{30}$$

Substituting Eqs. (30) and (6) into Eq. (29) and integrating one obtains

$$\Pi = \frac{1}{4\omega}\left(A_{11}\omega^2 + \left(\frac{\pi}{h}\right)^2 A_{55}\right)U^2 - 2NU \tag{31}$$

where

$$A_{11} = \int_0^h Q_{11}(z)\cos^2\frac{\pi z}{h}\mathrm{d}z, \qquad A_{55} = \int_0^h Q_{55}(z)\sin^2\frac{\pi z}{h}\mathrm{d}z \tag{32}$$

Minimization of the total energy with respect to the decay parameter ω yields

$$\omega = \frac{\pi}{h}\sqrt{\frac{A_{55}}{A_{11}}} \tag{33}$$

The substitution of Eq. (33) into Eq. (31) and minimization with respect to U results in the solution

$$U = \frac{2N}{\left(\frac{\pi}{h}\right)\sqrt{A_{11}A_{55}}} \tag{34}$$

Accordingly, Eq. (14) yields the following rotational elastic constraint coefficient for a unit-width section, accounting for a nonuniform temperature:

$$K = \frac{\pi h\sqrt{A_{11}A_{55}}}{4} \tag{35}$$

Note that the rotational restraint obtained from Eq. (35) differs for two legs since the temperature distribution is also different. Accordingly, it may be convenient to operate with two different values for legs a and b (Fig. 3), i.e. K_a and K_b.

The analysis of deformations of the delaminated legs of Section 1 can now be conducted. Even if a temperature gradient through the thickness of each leg is the same, thermally-induced moments will differ since different absolute values of temperature result in different material properties for each leg. The difference between two legs is identified by subscripts a (upper leg) and b (lower leg).

First of all, it is necessary to modify the reaction of z-pins to deformations of the legs. This reaction is given by an expression similar to Eq. (5), i.e.

$$p = K_0 - K_1(w_a + w_b) \tag{36}$$

Let us assume that the effect of temperature on the interfacial shear strength can be either disregarded or averaged through the depth of DCB. In this case, the expressions for K_0 and K_1 are evident from the previous discussion.

It is necessary to consider deformation of both legs of Section 1. Using the technical theory of beams, one can write the following equations of equilibrium for DCB of width b:

$$\frac{d^2M_i}{dx^2} = pb \tag{37}$$

where $i=a,b$ and

$$M_i = -D_i w_{i,xx} - M_i^T, \qquad D_i = b\int_0^h E_i(z)z^2\,dz, \tag{38}$$

$$E_i(z) = f[T_i(z)]$$

In Eq. (38), D_i is the stiffness of the ith leg that is affected by temperature and is a thermally-induced bending moment acting on the corresponding leg. The latter moment is independent of the axial coordinate. Accordingly, coupled equations of equilibrium obtained by substituting Eqs. (38) and (36) into Eq. (37) become

$$\begin{aligned} D_a\frac{d^4w_a}{dx^4} - K_1(w_a + w_b)b + K_0 b = 0,\\ D_b\frac{d^4w_b}{dx^4} - K_1(w_a + w_b)b + K_0 b = 0 \end{aligned} \tag{39}$$

The solution of these coupled differential equations should satisfy the following boundary conditions (for convenience, the coordinate system is chosen as in Fig. 5):

$$\begin{aligned} &w_a(0) = w_b(0) = 0 \qquad K_i b w_{i,x}(0) = -D_i w_{i,xx}(0) - M_i^T\\ &D_i w_{i,xx}(a) + M_i^T = 0 \quad -D_i w_{i,xxx}(a) = P \end{aligned} \tag{40}$$

Obviously, there are eight constants of integration in the solution of Eq. (39). These constants can be determined from eight conditions (40).

The solution of Eq. (39) can be obtained by reducing the system to one eighth-order differential equation. For example, eliminating w_b one obtains

$$\frac{D_a D_b}{K_1 b}\frac{d^8w_a}{dx^8} - (D_a + D_b)\frac{d^4w_a}{dx^4} = 0 \tag{41}$$

The solution of the system of Eq. (39) becomes

$$\begin{aligned} w_a &= A_0 + A_1x + A_2x^2 + A_3x^3 + A_4\sin\lambda x\\ &\quad + A_5\cos\lambda x + A_6\sinh\lambda x + A_7\cosh\lambda x,\\ w_b &= \frac{K_0}{K_1} - A_0 - A_1x - A_2x^2 - A_3x^3 + f(A_4\sin\lambda x\\ &\quad + A_5\cos\lambda x + A_6\sinh\lambda x + A_7\cosh\lambda x) \end{aligned} \tag{42}$$

where

$$\lambda = \sqrt[4]{\frac{(D_a + D_b)K_1 b}{D_a D_b}}, \qquad f = \frac{D_a\lambda^4}{K_1 b} - 1 \tag{43}$$

This represents the exact solution of the problem. An alternative solution could be obtained expanding the Kanninen approach that models the rotational stiffness of the beam through the introduction of an elastic foundation. The equations of equilibrium for each leg and for the affiliated half-depth of the intact section of DCB can easily be written as an extension of the previous paper [9]. The only explicit difference from the solution [9] is related to the presence of thermal terms. Implicitly, these equations of equilibrium are also different from [9] since temperature affects the values of material constants and the stiffness terms.

2.4. Analysis of the effect of a uniform temperature

If temperature is uniform, the properties of the material are also degraded uniformly throughout DCB. The solution

for the coefficient of rotational constraint of the intact section of DCB given by Eq. (18) for quasi-isotropic materials is valid, though the material constants in this expression should be modified to reflect the effect of temperature. Thermally-induced moments acting on the delaminated section of DCB are equal to zero. Accordingly, the only effect of temperature, besides the change in the stiffness of the intact section, will be through the magnitude of the stiffness of the legs in the delaminated section of DCB and the change in the interfacial shear strength τ.

The stiffness of polymer matrix and metal–matrix composites (PMC and MMC) invariably decreases with elevated temperature, implying larger deflections in DCB tests and an increased vulnerability to fracture and fatigue damage. The situation is different for CMC [21]. In particular, Nicalon-fiber/SiC-matrix orthotropic composites manufactured by DuPont illustrate a noticeable increase in the tensile modulus until temperature reaches 1000 °C, followed with an abrupt reduction of this modulus at higher temperatures. On the other hand, similar materials manufactured by another company (SEP) have a monotonous decrease of the tensile modulus in the entire range of temperatures from 0 to 1400 °C. Carbon/SiC orthotropic and quasi-isotropic CMC experience a moderate increase in the tensile modulus to about 1100 °C followed with a reduction of the modulus at higher temperatures (to 1600 °C). In SiC/SiC 2D composites, the stiffness is little affected by temperature, the tensile modulus increasing from 90 GPa at 23 °C to 100 GPa at 1000 °C.

The effect of an elevated temperature on the interfacial strength between z-pins and the material of layers can be rather significant, the strength often increasing with temperature. Accordingly, the stiffness of the equivalent elastic foundation provided by z-pins increases. This implies that the effectiveness of z-pins often increases with a uniform temperature.

2.5. Numerical examples

Eight composite DCB were considered in the examples analyzing the effect of transverse deflections in the thickness direction on the rotational restraint coefficient, i.e. the applicability of equation Eq. (18). The properties of these materials are presented in Table 1 that also shows the ratio r calculated according to Eq. (19). As follows from Table 1, the ratio remains close to unity for all considered materials. Moreover, in the presence of z-pins, the stiffness of the material in the thickness (z) direction increases. Therefore, the ratio r for z-pinned DCB is even closer to unity than that for DCB without z-pins. Accordingly, it is possible to evaluate the rotational stiffness of the intact section from Eq. (18), neglecting the changes in the thickness of the intact section.

The materials analyzed in the following examples include carbon/epoxy AS/3501 (properties presented in Table 1) and a unidirectional SiC/CAS ceramic matrix composite material with $E_x = 140$ GPa, $E_z = 130$ GPa, $G_{xz} = 60$ GPa, $\nu_{xz} = 0.3$. Two types of z-pins were considered. Carbon z-pins of the radius equal to 0.6 mm and the modulus of elasticity equal to 190 GPa were analyzed in SiC/CAS CMC DCB. Carbon/epoxy DCB were considered with titanium z-pins. These z-pins had the radius equal to 0.47 mm and the modulus of elasticity equal to 119 GPa. In all examples, geometry of DCB was such that $b = 20$ mm, $h = 2.19$ mm.

The comparison between the solution that accounts for the rotational stiffness of the intact section of DCB obtained from the theory of elasticity (presented in this paper) and the solution that employs an elastic foundation to model this stiffness [9] is presented in Fig. 6. As follows from this figure, two solutions yield the results for the deflection of the loaded (delaminated) end and the compliance of DCB that are in close agreement. The advantage of the present solution is in its relative simplicity and a more logical approach to the formulation of the problem. Predictably, a higher volume fraction of z-pins results in a decrease in deflections and compliance. This illustrates the effectiveness of z-pins for the enhancement of fracture resistance of joints working in Mode I conditions.

The deflections of the free end become equal to zero at a certain volume fraction of z-pins and the subsequent increase in the z-pin volume fraction actually produces negative deflections. This is due to exceedingly high total stiffness of the foundation. Naturally, negative deflections are physically impossible. Instead, zero deflections should be identified with a complete arrest of the crack. Such phenomenon was reported for z-pinned laminates by Rugg et al. [8] who noticed a change from delamination mode of

Table 1
Properties of materials considered in examples and the ratio r (Eq. 19)

Material	E_x (GPa)	E_x (GPa)	E_{xz} (GPa)	ν_{xz}	r
AS/3501 Cr/Ep	138.0	9.0	6.9	0.30	0.948
Scotchply® 1002 glass/epoxy	38.6	8.27	4.14	0.26	0.954
E-glass/vinylester	24.4	6.87	2.89	0.32	0.965
E-glass/polyester	34.7	8.5	4.34	0.27	0.951
E-glass/vinylester plain-weave	24.8	8.5	4.2	0.28	0.948
E-glass/epoxy eight-harness satin weave	25.6	15.6	5.4	0.283	0.964
2/2 twill carbon woven fabric/epoxy	49.38	8.18	3.09	0.44	0.982
2/2 twill carbon/aramid woven fabric/epoxy	35.86	6.76	2.70	0.446	0.979

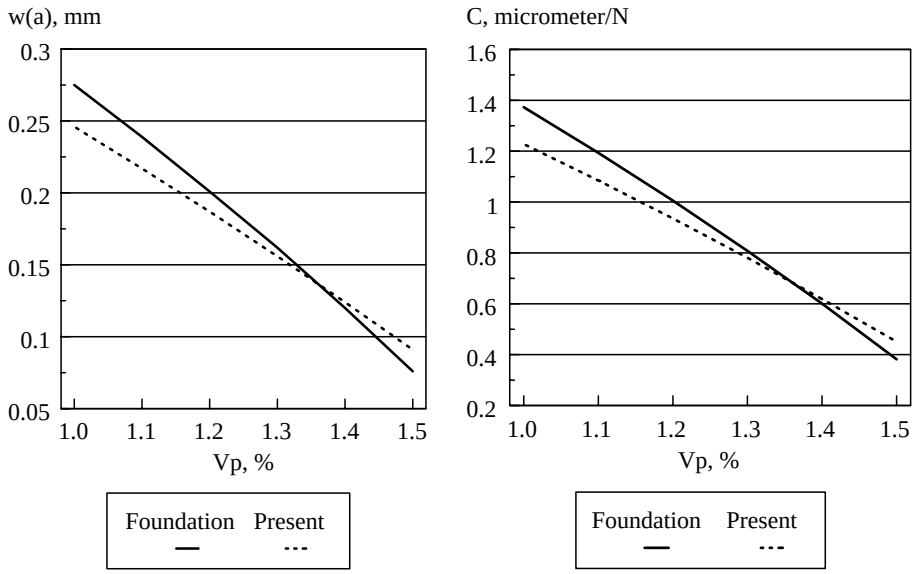

Fig. 6. Effect of z-pin volume fraction on the deflection of the loaded (delaminated) end and compliance of a SiC/CAS CMC DCB. The length of the crack is $a=20$ mm, the applied force is $P=400$ N. Rotational constraint provided by the intact section of DCB is found from the elasticity solution (Present) and from the elastic foundation method [9] (Foundation).

failure to microbuckling as a result of the introduction of z-pins. Notably, even a very small volume fraction of z-pins is sufficient to either drastically reduce deflections or completely arrest the crack. This volume fraction becomes particularly small, if the difference between the modulus of elasticity of the composite material and that of the pins increases (of course, the latter modulus is always larger).

The effect of the length of the crack on the response of SiC/CAS DCB calculated using the elasticity solution for the rotational constraint coefficient is shown in Fig. 7 for various z-pin volume fractions. The deflections of DCB with z-pin volume fractions equal to 0.8 and 1.0% abruptly increased at the crack lengths exceeding 30 mm. This occurs because z-pins are pulled out of the delaminated end of the DCB and it fails. On the other hand, DCB with z-pin volume fractions equal to 1.2% exhibited a reduction of deflections at $a>25$ mm. Therefore, the crack propagation was arrested in the specimen with this z-pin volume fraction at the crack length equal to 25 mm. Similar conclusions were obtained for carbon/epoxy AS4/3501-6 DCB, as shown in Fig. 8.

It is necessary to emphasize that the applicability of the present solutions should be analyzed keeping in mind a possible loss of strength and matrix cracking in the cantilever section of DCB. A quick estimate of the strength conducted by analyzing this section as a cantilever subject to the end lateral force illustrated that this mode of failure does not occur in carbon/epoxy DCB under consideration.

The situation is different in the case of a SiC/CAS specimen. This is related to the emergence of bridging matrix cracks perpendicular to the fibers. In case of bending of a delaminated cantilevered leg of DCB, these cracks will first form in the layers on the tensile surface of the leg (Section 1), at $x=0$. The matrix cracking stress for the material considered in the examples is close to 285 MPa. It is easy to estimate that the onset of the cracks in the fully clamped section will occur at the force $P=356$ N. However, in reality, the applied force corresponding to matrix cracking should be higher since the 'clamped end' of Section 1 is actually elastically constrained against rotations, i.e. the results shown in the paper are still reliable. Besides, bridging cracks do not significantly degrade the stiffness, so that the qualitative results shown in this paper would not be affected by their presence.

In general, as the cracks become longer, one of two tendencies dominates. The deflections may become so large that z-pins will be pulled out of Section 1. In this case, the rate of change in the compliance abruptly increases implying immediate failure. On the other hand, if the force is not sufficiently large, the crack can be arrested (in the present analysis, this is associated with a reduction of the deflections).

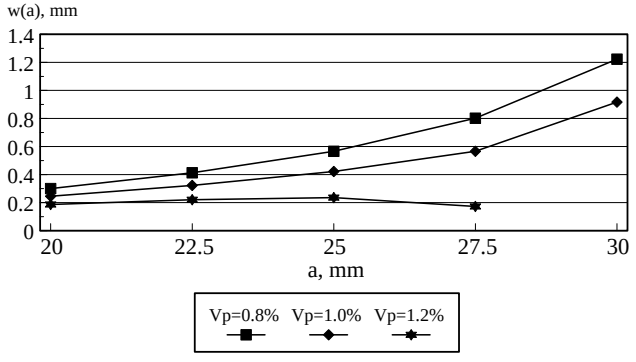

Fig. 7. Effect of the length of the crack on deflections of the delaminated end of a SiC/CAS DCB. The applied force is $P=400$ N.

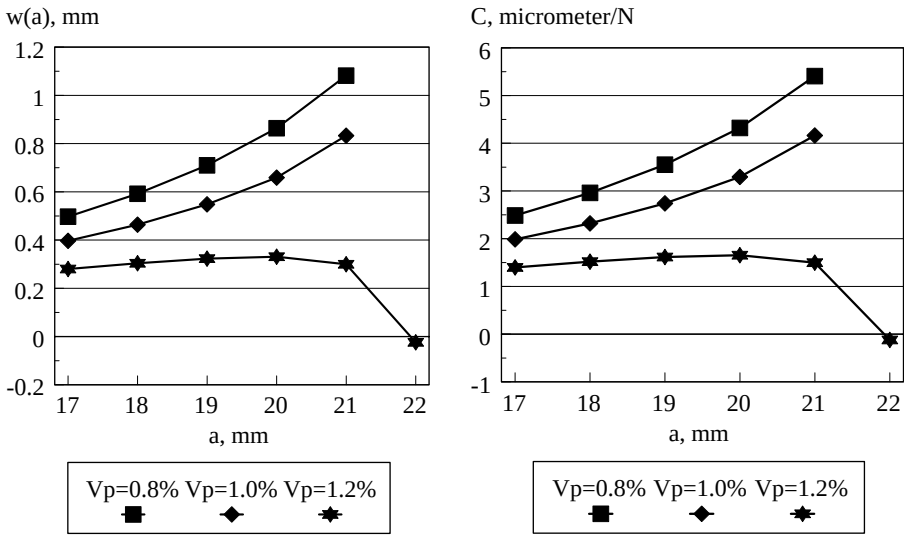

Fig. 8. Effect of the length of the crack on the deflection of the delaminated end of carbon/epoxy (AS4/3501-6) DCB and on its compliance. The applied force is $P=400$ N.

The analytical evaluation of the rate of change of compliance and subsequently, the strain energy release rate are impractical, in the presence of z-pins. Therefore, in agreement with the recommendation of Rugg et al. [8], fracture toughness is not recommended for the characterization of z-pinned joints. Instead, the maximum deflection of the delaminated section of the joint can be used to characterize their efficiency, understanding that the joints failure can be associated with complete pullout of z-pins from the legs.

The effect of the applied force on the deflections and compliance is illustrated in Fig. 9 for a SiC/CAS specimen. The results were generated using the elastic foundation approach to modeling the rotational restraint provided by the intact section of DCB [9]. Although the results may be affected by matrix cracking on the tensile surface, but the general tendencies are obvious. Deflections increase almost proportionally to the magnitude of the applied force (if the length of the crack is constant). The compliance also increases with larger forces. Although the rate of this increase in compliance is reduced at large values of the applied force, matrix cracking may avert this tendency and result in larger compliance values.

The effect of a uniform temperature discussed in the corresponding section of this paper is reflected in both the changes in the stiffness as well as the change in the interfacial shear strength. The former effect is anticipated to be relatively smaller, at least in CMC joints. Therefore,

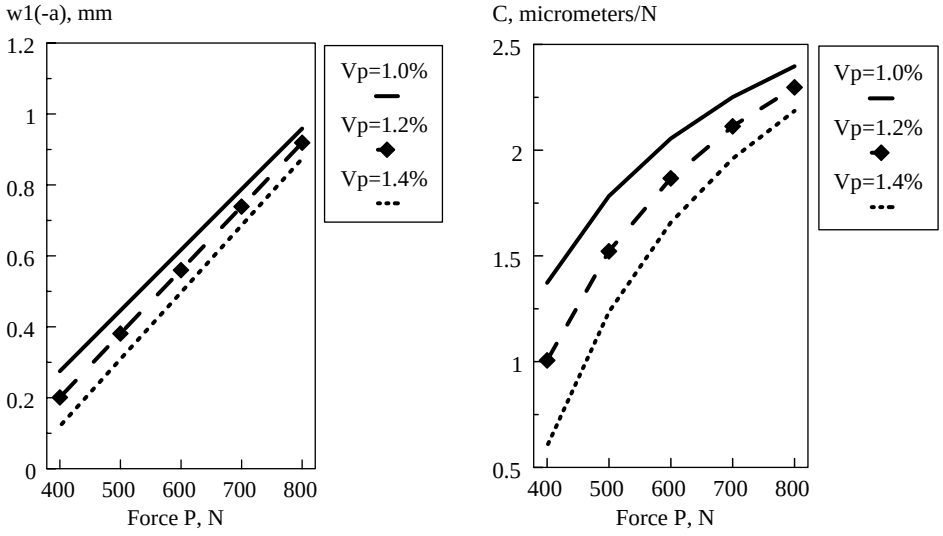

Fig. 9. Effect of the applied force on the deflections of the delaminated end and compliance of SiC/CAS DCB. The length of the crack is $a=20$ mm.

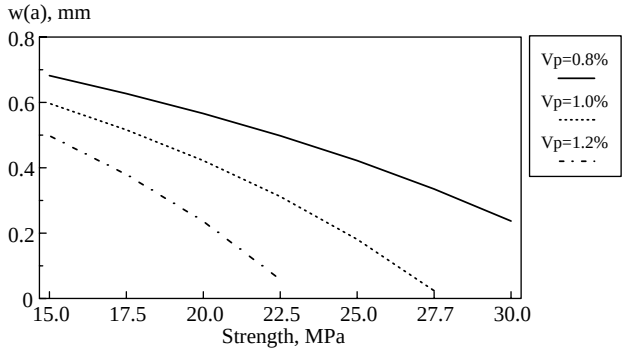

Fig. 10. Effect of the interfacial shear strength between the z-pin and composite material of the SiC/CAS DCB on the deflections of the delaminated end. The length of the crack is 25 mm. The applied force is $P=400$ N.

the following examples illustrate the influence of the magnitude of the interfacial shear strength between z-pins and composite material of DCB on the deflections of the delaminated and of DCB and accordingly, on its fracture. This effect is illustrated for three different z-pin volume fractions for a SiC/CAS CMC DCB in Fig. 10. As is shown in this figure, even a modest increase in the interfacial shear strength results in an abrupt reduction in the deflections of the delaminated end of DCB. This conclusion is further reinforced by results shown for CMC and carbon/epoxy DCB in Figs. 11 and 12 where the changes in deflections are depicted as functions of the crack propagation (crack length). The arrest and failure cases are clearly observed in these figures and it is evident that even a modest increase in the interfacial shear strength can alter the response from delamination failure to the arrest of the crack.

A large effect of the interfacial shear strength between z-pins and the material of the joint discussed above implies that the resistance to fracture and fatigue damage can be enhanced by increasing the interfacial strength. Besides increased temperature, this goal might be achieved by using

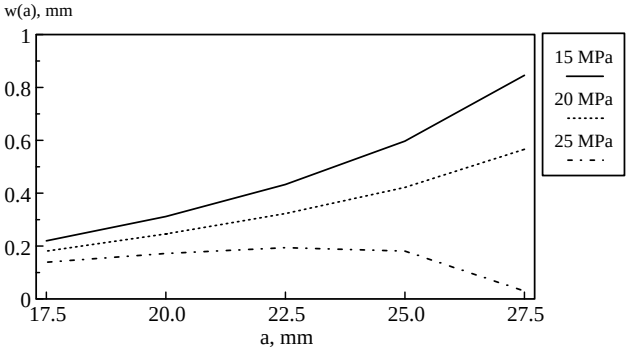

Fig. 11. Effect of the interfacial shear strength between the z-pin and composite material of the SiC/CAS DCB on the change in deflections of the delaminated end as a function of the length of the crack. The volume fraction of z-pins is equal to 1%. The applied force is $P=400$ N.

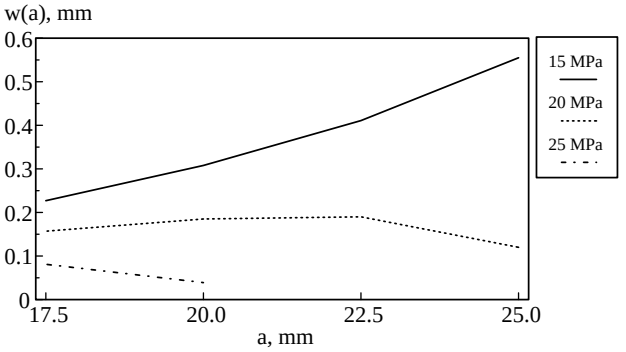

Fig. 12. Effect of the interfacial shear strength between the z-pin and composite material of the plain-woven AS4/3501-6 carbon/epoxy DCB on the change in deflections of the delaminated end as a function of the length of the crack. The volume fraction of z-pins is equal to 1%. The applied force is $P=400$ N.

a rougher surface of z-pins. In particular, if z-pins for CMC joints are formed from ceramic fibers, these fibers may be interwoven producing a rough surface (similar to steel reinforcements presently analyzed in so-called steel-reinforced polymers shown in Fig. 13). This approach would increase the resistance to a relative slip between the z-pin and the material of the joined layers providing a higher degree of interconnection and therefore, a higher resistance to pullout and fracture. A potential weakness of the proposed approach may be related to local microstress concentrations and microcracking. Obviously, experimental work in this area is well warranted due to potential advantages of the method.

2.6. Conclusions and recommendation

Although the analysis was conducted on the example of a representative DCB, the following conclusions are applicable to co-cured z-pinned joints of an arbitrary geometry.

1. Z-Pins represent an effective tool of suppression of Mode I delamination fracture in co cured joints.
2. The arrest of cracks associated with using z-pins occurs at a relatively short length of the crack. If z-pins are not effective in preventing fracture, the failure can be

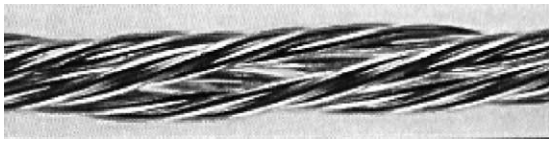

Fig. 13. Steel cord produced by twisting two-wire strands around three-wire strands in steel–reinforced plastics. A similar geometry may be adopted for z-pins formed of fibers to enhance the interfacial properties and reduce z-pin pullout (from the paper ‘Properties and potential for application of steel reinforced polymer (SRP) and steel reinforced grout (SRG) composites’ by X. Huang, V. Birman, A. Nanni, G. Tunis. Composites Part B: Engineering, Vol. 36, pp. 73–82, 2005).

associated with the onset of the process of complete pullout of z-pins from the material.

3. It is difficult to analytically evaluate the fracture toughness in the presence of z-pins. Instead, it is easier to assess the effectiveness of z-pins by monitoring a characteristic displacement, such as the deflection of the loaded end of the delaminated section of DCB. In this case, the arrest of the crack can be associated with $dw/da = 0$. If this condition is achieved, the deflection obtained by the analytical solution decreases for a longer crack due to the overwhelming reaction of z-pins. Physically, such decrease is impossible, i.e. the above condition implies the arrest of the crack.
4. A new method of the analysis of DCB based on the estimate of the rotational stiffness of the intact section through the solution of the elasticity problem provides an accurate and logical estimate of the effect of this section on deformations of delaminated legs of DCB and their failure.
5. Transverse shear deformations of delaminated legs of DCB may affect the solution only if the length of the crack is very small. Although cracks in z-pinned DCB either fail or are arrested when they are relatively short, the slender (technical) beam theory provides an accurate estimate of the effectiveness of DCB in most cases.
6. As was found in representative examples, the arrest of delamination cracks occurred even when the volume fraction of z-pins was quite small (typically, in the range between 1 and 1.5%).
7. Elevated temperature may result in an increase of the interfacial strength between z-pins and composite layers. This might make z-pinned joints even more efficient in high-temperature applications than at room temperature.
8. Besides the effect on the interfacial shear strength, temperature affects the properties of the composite material of the joint. These two effects are often opposite: for example, a higher interfacial strength due to an elevated temperature is beneficial, while a lower stiffness and strength of the joined layers are detrimental for the integrity of the joint.
9. It should be noted that even if elevated temperature improves both the interfacial shear strength as well as the stiffness of the joint material, it might still be detrimental to a CMC joint. This is related to oxidation of fiber–matrix interfaces that occurs at an elevated temperature as a result of oxygen transmitted to the interface through cracks in a ceramic matrix. Such oxidation is accompanied by an abrupt embrittlement of the material.
10. Even a relatively small increase of the interfacial shear strength between the z-pin and composite, whether caused by an elevated temperature or resulting from a choice of materials or technological process, is beneficial for the integrity of the joint. An interesting practical recommendation from this conclusion is related to a possible design of the surface of z-pins. If a z-pin is manufactured from fibers, a woven configuration resulting in a rough surface with a potentially better 'grasp' between the z-pin and composite material may be useful. A drawback of such approach is related to unavoidable microscopic stress concentrations and interfacial cracks. Nevertheless, experimental studies of 'rough' z-pin surfaces should be conducted since a possible benefit for the prevention and arrest delamination cracks is significant.

In general, using z-pins in CMC joints subject to Mode I fracture loading greatly improves the integrity of the joint. A very small volume fraction of z-pins can result in the arrest of delamination cracks.

Acknowledgements

This research was supported by the Air Force Office for Scientific Research Contract F33615-98-D-3210.

References

[1] Freitas G, Magee C, Dardzinski, Fusco T. Fiber insertion process for improved damage tolerance in aircraft laminates. J Adv Mater 1994; 25:36–43.
[2] Barrett DJ. A micromechanical model for the analysis of Z-fiber reinforcement. AIAA paper, AIAA-96-1329-CP; 1996.
[3] Lin CY, Chan WS. Stiffness of composite laminates with Z-fiber reinforcement. AIAA paper AIAA-99-1294; 1999.
[4] Palazotto AN, Gummadi LNB, Vaidya UK, Herup EJ. Low velocity impact damage characteristics of Z-fiber reinforced sandwich panels—an experimental study. Compos Struct 1999;43:275–88.
[5] Vaidya UK, Kamath MV, Hosur MV, Mahfuz H, Jeelani S. Low velocity impact response of cross-ply laminated sandwich composites with hollow and foam-filled Z-pin reinforced core. J Compos Technol Res 1999;21:84–98.
[6] Mabson GE, Deobald LR. Design curves for 3D reinforced composite laminated double cantilever beams. In: Rajapakse YDS, Kardomateas GA, Birman V, editors. Mechanics of sandwich structures, AD-vol. 62/AMD-vol. 245. New York: American Society of Mechanical Engineers; 2000. p. 89–99.
[7] Freitas G, Fusco T, Campbell T, Harris J, Rosenberg S. Z-fiber technology and products for enhancing composite design. AGARD Conf Proc 1996;17:1–8.
[8] Rugg KL, Cox BN, Massabo R. Mixed mode delamination of polymer composite laminates reinforced through the thickness by Z-fibers. Compos Part A 2002;33:177–90.
[9] Byrd LW, Birman V. The estimate of the effect of Z-pins on the strain energy release rate, fracture and fatigue in a composite co-cured Z-pinned double cantilever beam. Compos Struct 2005;68:53–63.
[10] Kanninen MF. An augmented double cantilever beam model for studying crack propagation and arrest. Int J Fract 1973;9:83–92.
[11] Kanninen MF. A dynamic analysis of unstable crack propagation and arrest in the DCB test specimen. Int J Fract 1974;10:415–30.

[12] Gehlen PC, Popelar CH, Kanninen MF. Modeling of dynamic crack propagation: I. Validation of one-dimensional analysis. Int J Fract 1979;15:281–94.
[13] Williams JG. End correction for orthotropic DCB Specimens. Compos Sci Technol 1989;35:367.
[14] Ozdil F, Carllson L. Beam analysis of angle-ply laminate DCB specimens. Compos Sci Technol 1999;59:305–15.
[15] Penado FE. A closed form solution for the energy release rate of the double cantilever beam specimen with an adhesive layer. J Compos Mater 1993;27:383–407.
[16] Birman V, Byrd LW. Strain energy release rate of co-cured Z-pinned composite double cantilever beams. ASCE J Aerospace Eng; in press.
[17] Li VC. Postcrack scaling relations for fiber reinforced cemenitious composites. J Mater Civil Eng 1992;4:41–57.
[18] Chamis CC. Simplified composite micromechanics equations for hygral, thermal and mechanical properties. SAMPE Q 1984;15(3): 14–23.
[19] Vinson JR. The behavior of sandwich structures of isotropic and composite materials. Lancaster, Pennsylvania: Technomic; 1999.
[20] Birman V. Effect of elevated temperature on wrinkling in composite sandwich panels Proceedings of the 18th annual SAMPE meeting; 2004.
[21] Schwartz MM. Composite materials, volume I: properties, non-destructive testing, and repair. Upper Saddle River, NJ: Prentice- Hall; 1996.